Cancer Cell
Article

Siah2-Dependent Concerted Activity of HIF and FoxA2 Regulates Formation of Neuroendocrine Phenotype and Neuroendocrine Prostate Tumors

Jianfei Qi,[1] Koh Nakayama,[2] Robert D. Cardiff,[3] Alexander D. Borowsky,[3] Karen Kaul,[4,5] Roy Williams,[1] Stan Krajewski,[1] Dan Mercola,[6] Philip M. Carpenter,[6] David Bowtell,[7] and Ze'ev A. Ronai[1,*]
[1]Signal Transduction Program, Sanford-Burnham Medical Research Institute, La Jolla, CA 92037, USA
[2]MTT program, Medical Research Institute, Tokyo Medical and Dental University, Tokyo 113-8510, Japan
[3]Center for Comparative Medicine and Department of Pathology, School of Medicine, University of California, Davis, CA 95616, USA
[4]NorthShore University Health System, Evanston Hospital, Evanston, IL 60201, USA
[5]Pritzker School of Medicine, University of Chicago, Chicago, IL 60637, USA
[6]Translational Cancer Biology, University of California, Irvine, CA 92697, USA
[7]Research Division, Peter McCallum Cancer Centre, Melbourne 8006, Victoria, Australia
*Correspondence: ronai@sanfordburnham.org
DOI 10.1016/j.ccr.2010.05.024

SUMMARY

Neuroendocrine (NE) phenotype, seen in >30% of prostate adenocarcinomas (PCa), and NE prostate tumors are implicated in aggressive prostate cancer. Formation of NE prostate tumors in the *TRAMP* mouse model was suppressed in mice lacking the ubiquitin ligase Siah2, which regulates HIF-1α availability. Cooperation between HIF-1α and FoxA2, a transcription factor expressed in NE tissue, promotes recruitment of p300 to transactivate select HIF-regulated genes, *Hes6*, *Sox9*, and *Jmjd1a*. These HIF-regulated genes are highly expressed in metastatic PCa and required for hypoxia-mediated NE phenotype, metastasis in PCa, and the formation of NE tumors. Tissue-specific expression of FoxA2 combined with Siah2-dependent HIF-1α availability enables a transcriptional program required for NE prostate tumor development and NE phenotype in PCa.

INTRODUCTION

Prostate cancer is the second leading cause of cancer deaths among men in Western nations. Among the metastatic forms of prostate adenocarcinoma (PCa) are those that express neuroendocrine (NE) markers, often referred to as neuroendocrine differentiation (NED) or NE phenotype. NED is seen in >30% of PCa and is associated with poor prognosis and androgen independence (Cindolo et al., 2007). A small percentage (0.5%–2%) of human prostate tumors develop as highly aggressive NE tumors, which have a 35% survival rate in 2 years (Cindolo et al., 2007; Sella et al., 2000). Factors implicated in NED of LNCaP prostate cancer cells in vitro include IL-6 treatment (Deeble et al., 2001), androgen removal (Yuan et al., 2006), and ionizing radiation (Deng et al., 2008). In transgenic animals, T antigen expression or inactivation of p53 and Rb has been associated with prostate NE tumors (Huss et al., 2007; Zhou et al., 2006).

FoxA2, a member of the FoxA subfamily of Forkhead box transcription factor, is expressed in mouse prostate NE carcinomas (Chiaverotti et al., 2008; Mirosevich et al., 2006) and NE foci of human PCa (Mirosevich et al., 2006). HIF-1α, the master regulator of the hypoxia response, is also expressed in NE tumors (Monsef et al., 2007). HIF-1α is regulated under normoxia by the E3 ligase pVHL and is also regulated under mild hypoxia (2%–5% O_2) by the ubiquitin ligase Siah2. Siah2 controls prolyl

Significance

Prostate adenocarcinomas (PCa) with neuroendocrine (NE) phenotype and NE prostate tumors are associated with poor prognosis and androgen independence. Here, we demonstrate that formation of NE tumors and metastasis of PCa require the ubiquitin ligase Siah2. Through its role in the control of HIF-1α availability, Siah2 enables cooperation between HIF-1α and the NE-specific transcription factor FoxA2. Genes induced by HIF-1α/FoxA2 cooperation are expressed in NE lesions and in metastatic human PCa and required for formation of the NE phenotype, for metastasis of human PCa, and for the development of NE tumors. Tissue-specific cooperation between transcription factors that promote NE phenotype and prostate tumor development offers a paradigm for the development, progression, and potential targeting of aggressive prostate tumors.

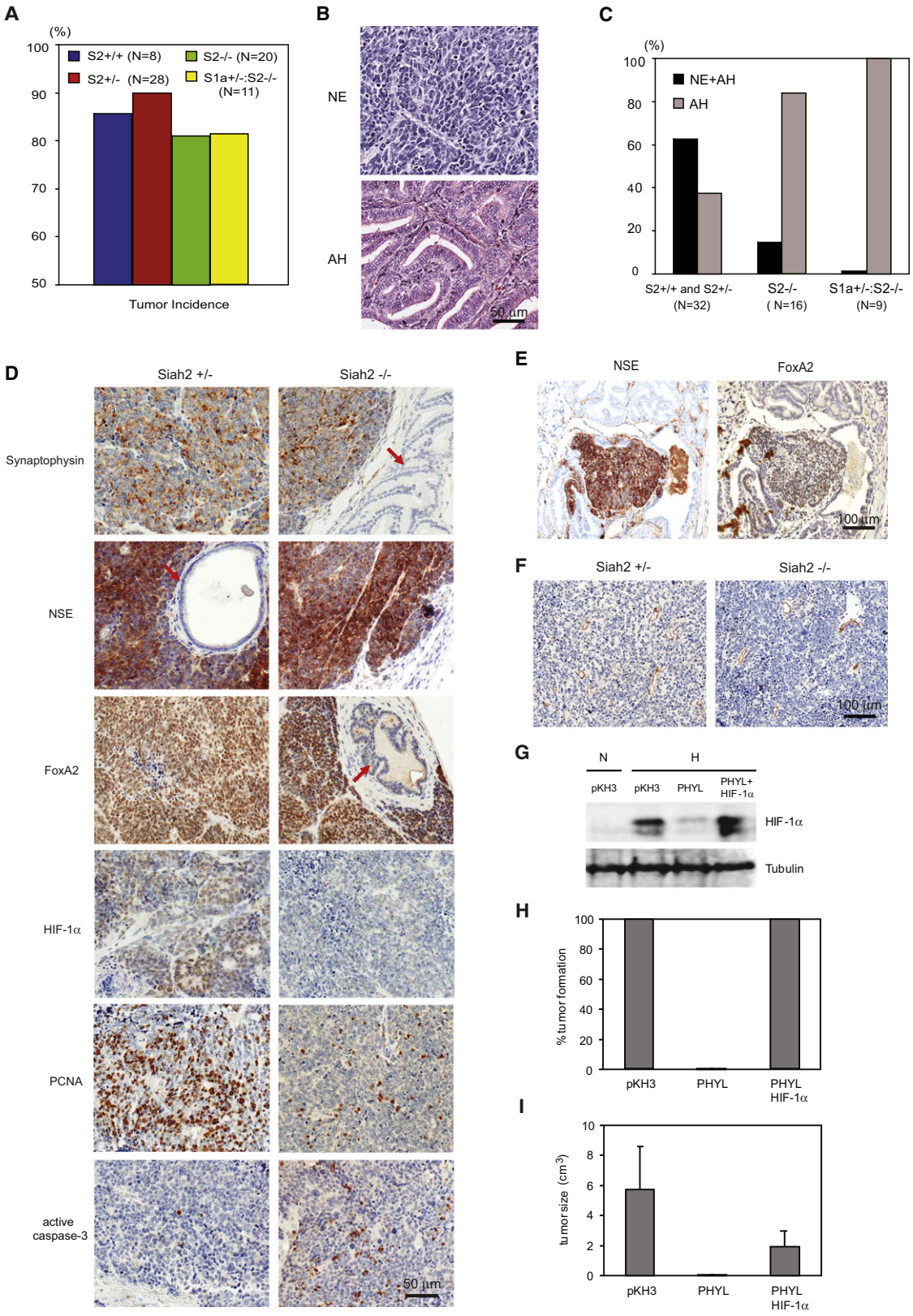

Figure 1. Tumorigenesis in *TRAMP*^{Tg}/*Siah2* Mice

(A) Primary tumor incidences of *TRAMP* mice with indicated *Siah2* genotype are shown as percentages.

(B) Typical H&E staining of neuroendocrine carcinoma (NE) derived from *TRAMP/Siah2*$^{+/-}$ and AH derived from *TRAMP/Siah2*$^{-/-}$ mice.

hydroxylase 1/3 (PHD) stability (Nakayama et al., 2004), thereby affecting PHD availability to modify HIF-1α, which is essential for HIF-1α's association with and ubiquitination by pVHL (Ivan et al., 2001). Given that PHD functions as cellular oxygen sensors (Aragones et al., 2009; Nakayama et al., 2009), Siah2 is expected to play a central role in controlling hypoxia and related biological outcomes, including tumorigenesis and metastasis (Nakayama et al., 2009). Indeed, inhibition of Siah2 activity blocks formation of tumors (Ahmed et al., 2008; Moller et al., 2009; Qi et al., 2008; Schmidt et al., 2007). Further, Siah2's contribution to melanoma metastasis is HIF dependent (Qi et al., 2008).

Once stabilized, HIF-1α translocates to the nucleus and dimerizes with HIF-1β; the heterodimers then bind to hypoxia responsive elements (HREs) to regulate transcription of hypoxia-responsive genes (Semenza, 2003). Several transcription factors cooperate with HIF to regulate its transcriptional activity; HIF activity is enhanced by β-catenin (Kaidi et al., 2007) and repressed by FOXO3a (Emerling et al., 2008). HIF can also modulate activity of other transcriptional regulators: HIF-1α potentiates Notch signaling (Gustafsson et al., 2005) and represses c-Myc activity (Zhang et al., 2007).

Given the role of Siah2 in regulation of HIF-1α, we set to determine its role in prostate cancer development and metastasis.

RESULTS

Attenuated Formation of Prostate NE Carcinoma in *Siah2* Null *TRAMP* Mice

We employed the *TRAMP* mouse model, in which prostate-specific expression of SV40 T antigen results in prostate tumors that metastasize to lymph nodes, lung, and liver (Gingrich et al., 1996), to assess the possible role of Siah in tumor growth and metastasis. Analysis of 8-month-old *TRAMP* mice with different *Siah2* background (*TRAMP*/*Siah2*$^{-/-}$, *TRAMP*/*Siah2*$^{+/-}$, and *TRAMP*/*Siah2*$^{+/+}$) revealed that the majority developed prostate masses (Figure 1A). Most primary masses were composed of benign proliferations of stroma and epithelium with atypical epithelial hyperplasia (AH) in *TRAMP*/*Siah2*$^{-/-}$ mice, compared with a preponderance of NE carcinoma in the *TRAMP*/*Siah2*$^{+/-}$ and *TRAMP*/*Siah2*$^{+/+}$ mice (Figures 1B and 1C). Although *TRAMP* AH have been referred to as adenocarcinoma in some literature (e.g., Gingrich et al., 1996), we refer them as *TRAMP* AH in lieu of clear discrimination, detailed in Chiaverotti et al., (2008). NE carcinomas were identified by morphology (Figure 1B) and expression of the well-established NE markers synaptophysin, neuron-specific enolase (NSE), and FoxA2 (Figure 1D), consistent with the notion that the *TRAMP* tumors are primarily of NE origin (Chiaverotti et al., 2008). In clear contrast, FoxA2, synaptophysin, and NSE were undetectable in normal prostate glands (Figure 1D, arrows) or in AH (data not shown).

Since Siah1 also contributes to the regulation of PHD and consequently HIF availability (Nakayama et al., 2004; Qi et al., 2008), we also evaluated Siah1a function in prostate tumor formation. *Siah2* and *Siah1a* doubly homozygous mutant mice are non-viable (Frew et al., 2003). We therefore established a *TRAMP*/*Siah1a*$^{+/-}$*Siah2*$^{-/-}$ mouse line. *TRAMP*/*Siah1a*$^{+/-}$ *Siah2*$^{-/-}$ mice showed a prostate tumor incidence similar to that seen in *TRAMP*/*Siah2*$^{-/-}$ mice (Figure 1A) but lacked NE tumors (Figure 1C).

In the *TRAMP* mice, the early NE tumor lesions develop in the ventral prostate after 3 months and are recognized as foci that express NE markers. To examine the effect of Siah2 on the development of early stage NE tumors, we analyzed 5-month-old mice. NE foci were identified in three of six control mice but in none of the ten *TRAMP*/*Siah2*$^{-/-}$ mice (Figure 1E; the difference is statistically significant). These data reveal that in the *TRAMP* model Siah is required for development of NE carcinomas.

AH predominantly develops in the dorsal lateral lobe of prostate and is identifiable in 1-month-old *TRAMP* mice (Chiaverotti et al., 2008). To evaluate whether Siah also involved in the progression of AH, we analyzed the dorsal prostate lobes from 1- and 3-month-old mice and found that lack of Siah2 delayed the progression from a normal prostate gland to the early and medium stages AH in 1-month-old mice and into the late-stage AH in the 3-month-old mice (Figures S1A and S1B available online).

Altered HIF-1α Expression Correlates with Reduced Cell Proliferation and Enhanced Cell Death in Primary NE Tumor from *TRAMP*/*Siah2*$^{-/-}$ Mice

Consistent with Siah2 regulation of HIF-1α availability, HIF-1α level was reduced in the very few NE carcinomas observed (Figure 1D) and in AH (Figure S1C) from *TRAMP*/*Siah2*$^{-/-}$ mice compared with *TRAMP*/*Siah2*$^{+/-}$ mice. HIF-2α staining was also reduced in AH from *TRAMP*/*Siah2*$^{-/-}$ mice (Figure S1C), whereas HIF-2α was undetectable in NE carcinoma from any genotype (data not shown). These findings are also consistent with the observation that HIF-1α but not HIF-2α is coexpressed with NE markers in prostate cancers (Monsef et al., 2007).

Potential changes in proliferation, apoptosis, and angiogenesis were evaluated with PCNA, TUNEL/active caspase-3, and CD31, respectively. NE tumors, but not AH, from *TRAMP*/*Siah2*$^{-/-}$ mice showed reduced cell proliferation and increased

(C) Incidence of NE and AH in *TRAMP* mice with indicated *Siah* genotypes. Number of mice for each genotype is indicated. Dark bars indicate NE+AH. $p < 0.005$ for NE tumor incidence between control and *Siah*-deficient *TRAMP* mice.
(D) IHC analyses of primary NE carcinoma with indicated genotypes using the indicated antibodies. Arrows indicate normal prostate epithelial tissues.
(E) NSE and FoxA2 staining of the NE tumor foci of 5-month-old *TRAMP* mice.
(F) IHC staining of CD31 in NE carcinomas from mice of indicated genotypes.
(G) Re-expression of HIF-1α in PHYL-expressing TRAMP-C cells. Cells were stably transfected with indicated expression vectors. PHYL-expressing cells were further stably transfected with HIF-1α and maintained in normoxia (N) or hypoxia (H) for 6 hr before analyses by western blotting for HIF-1α.
(H and I) TRAMP-C cells (3×10^6) expressing control pKH3 vector, PHYL, or PHYL+HIF-1α were injected subcutaneously into the flanks of nude mice. The frequency of tumor formation (H) and size of xenograft tumor (I) 8-weeks postinjection are shown. In (I), each column represents mean ± SD (standard deviation) for five mice, $p < 0.05$ for pKH3 versus PHYL+HIF-1α. See also Figure S1 and Table S1.

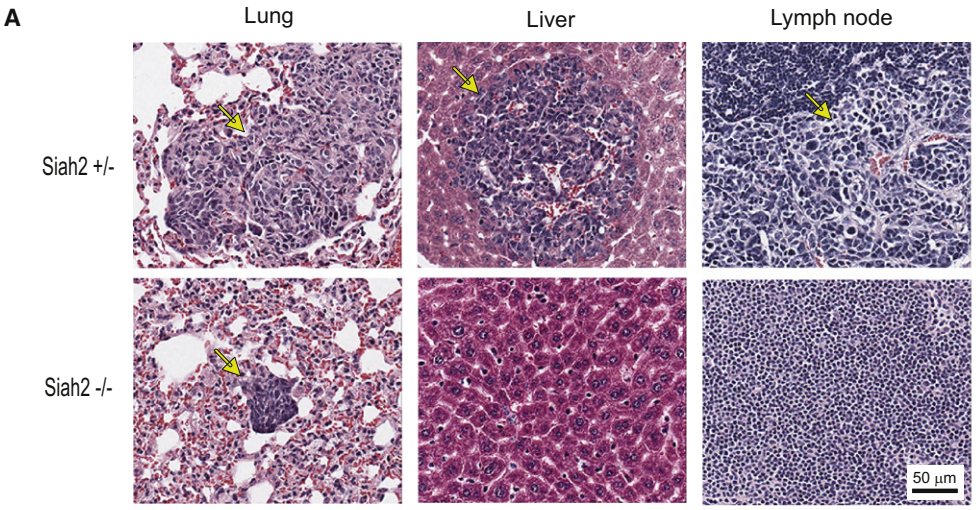
A
Lung
Liver
Lymph node
Siah2 +/-
Siah2 -/-
50 μm

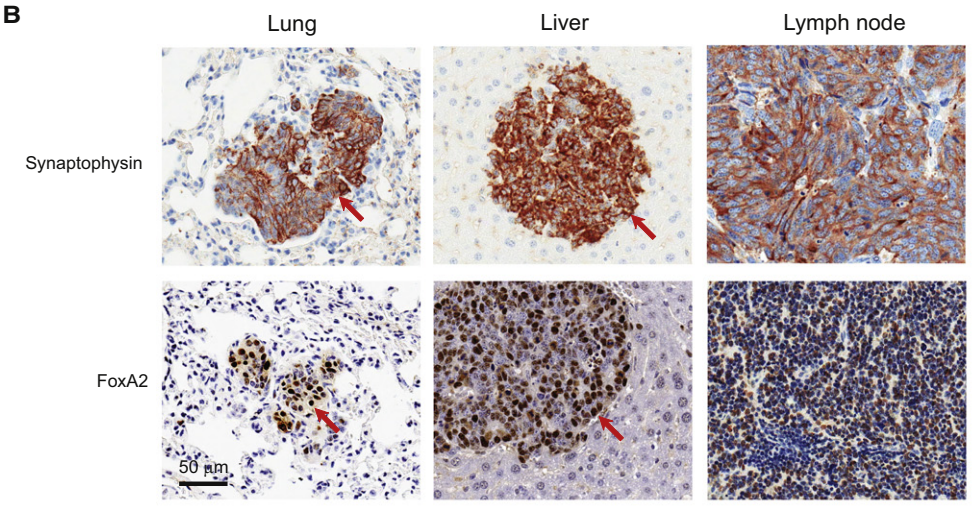
B
Lung
Liver
Lymph node
Synaptophysin
FoxA2
50 μm

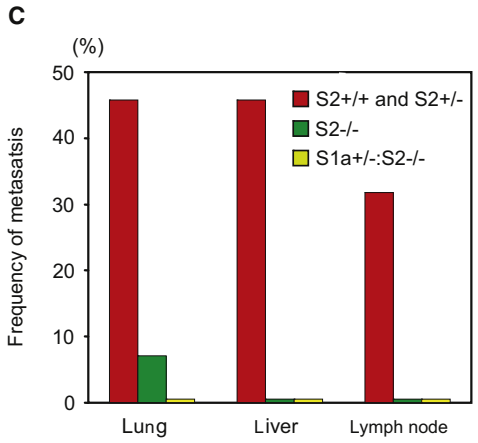
C
(%)
50
40
30
20
10
0
Frequency of metasatsis
S2+/+ and S2+/-
S2-/-
S1a+/-:S2-/-
Lung
Liver
Lymph node

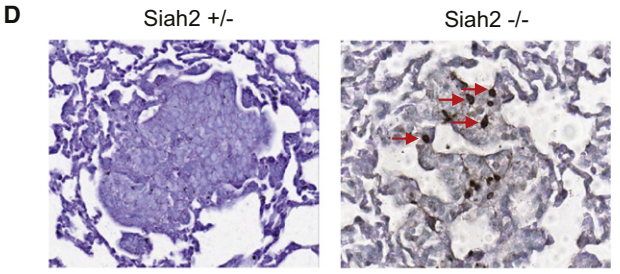
D
Siah2 +/-
Siah2 -/-

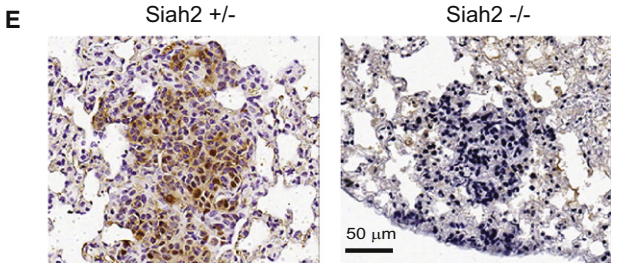
E
Siah2 +/-
Siah2 -/-
50 μm

apoptosis compared with those seen in *TRAMP/Siah2*$^{+/-}$ mice (Figure 1D; Figure S1C; Table S1). Vascular density was similar in the two strains in both the NE tumor (Figure 1F and Table S1) and AH (Figure S1C and Table S1). Hence, loss of Siah and consequent downregulation of HIF levels appear to specifically govern proliferation and cell survival of NE tumors.

To directly assess a possible role for Siah2 and HIF-1α in tumorigenesis of *TRAMP* cells, we analyzed TRAMP-C cells derived from *TRAMP* tumors (Foster et al., 1997). These cells likely represent NE tumor-derived cells as they express multiple NE specific transcription factors (Figure 4A and data not shown). The PHYL peptide binds to Siah's substrate recognition site (House et al., 2003) and attenuates Siah2's effect on PHD1/3 and thus reduces HIF-1α levels under hypoxia (Moller et al., 2009; Qi et al., 2008). Expression of the PHYL peptide in TRAMP-C cells effectively abolished their ability to form tumors (Figures 1H and 1I), consistent with the finding that NE tumors do not form in *TRAMP/Siah1a*$^{+/-}$*Siah2*$^{-/-}$ mice (Figure 1C). Forced HIF-1α expression in TRAMP-C cells expressing PHYL peptide by transfection (Figure 1G) partially recovered their ability to form tumors (Figures 1H and 1I). These data support the role of Siah2, in part through its regulation of HIF-1α levels, in formation of NE prostate tumors.

Reduced Metastasis in *TRAMP/Siah2*$^{-/-}$ Mice

Metastatic lesions in the liver, lung, and lymph nodes of *TRAMP* mice were identified as NE carcinomas, based on morphology (Figure 2A) and FoxA2/synaptophysin expression (Figure 2B). However, both the frequency and size of metastatic lesions were significantly reduced (6-fold) in the lung and were not found in liver and lymph nodes of *TRAMP/Siah2*$^{-/-}$ mice, compared with *TRAMP/Siah2*$^{+/-}$ or *TRAMP/Siah2*$^{+/+}$ animals (Figures 2A and 2C). Furthermore, we found no metastases in *TRAMP/Siah1a*$^{+/-}$*Siah2*$^{-/-}$ mice (Figure 2C). The very few lung metastases observed in *TRAMP/Siah2*$^{-/-}$ mice were smaller, showed reduced cell proliferation, and enhanced cell death (Figures 2D and 2E). These findings point to the role of Siah2 in *TRAMP* tumor metastasis.

FoxA2 Stimulates HIF Transcriptional Activity

Given that the NE-specific transcription factor FoxA2 is coexpressed with HIF-1α protein in nuclei of NE carcinoma cells (Figure 1D), we tested the possibility that these transcription factors cooperate with each other. While expression of exogenous FoxA2 in TRAMP-C cells did not alter the expression of an HRE-linked luciferase construct (HRE-Luc, data not shown), expression of exogenous HIF-1α alone elicited a modest increase in HRE-Luc activity as expected (Figure 3A). Significantly, coexpression of HIF-1α and FoxA2 led to a 6-fold increase in luciferase activity overexpression of HIF-1α alone (Figure 3A). Coexpression of IPAS, a spliced form of HIF-3α with potent dominant-negative activity toward all HIFs (Makino et al., 2002), or inhibiting HIF-1α expression by expressing S2RM (a dominant-negative form of Siah2) or PHYL abolished FoxA2-potentiated HRE-Luc activity (Figure 3A). Importantly, knockdown of FoxA2 caused a ~40% reduction in HRE-Luc activity under hypoxia, although the degree of inhibition was lower than that seen with HIF-1α or HIF-1β siRNA (Figure 3B and Figure S2A). These data establish a role for FoxA2 in enhancing HIF-mediated transcriptional activity. In contrast, HIF-1α did not stimulate FoxA2 transcription activity (data not shown), indicating that HIF/FoxA2 transcriptional synergy may be restricted to the context of an HRE. Notably, FoxA1 did not increase HRE-Luc activity in the presence of HIF-1α (data not shown).

We then mapped the FoxA2 domains required for cooperation with HIF-1α. FoxA2 fragments consisting of the N-terminal transactivation domain (N-TAD), the central forkhead domain, or the C-terminal transactivation domain (C-TAD) were generated and evaluated for their effect on FOXA- and HIF-1α-dependent transcription activity (Figure S2B). FoxA2 mutants lacking either the N-TAD or C-TAD exhibited FOXA-dependent transcriptional activity similar to that of the wild-type FoxA2 (Figure 3C), indicating that one transactivation domain is sufficient for FoxA2 transcriptional activity. FoxA2 mutants lacking the C-TAD promoted HIF-dependent transcriptional activity to a level similar to wild-type FoxA2, whereas the FoxA2 mutant lacking the N-TAD was much less effective (Figure 3D). The FoxA2 C terminus, which contains intrinsic chromatin remodeling activity (Cirillo et al., 2002), was dispensable for HRE activation (construct m-2 in Figure 3D; Figure S2B), thereby excluding the role of chromatin remodeling activity in FoxA2 cooperation with HIF. These data suggest that the N-TAD and forkhead domains of FoxA2 are required to stimulate HIF-mediated transcriptional activity.

HIF Interacts with FoxA2

Coexpression of HA-FoxA2 or HA-FoxA1 with Flag-HIF-1α in 293T cells followed by immunoprecipitation of Flag-HIF-1α identified HA-FoxA2, but not HA-FoxA1, as an HIF-associated protein (Figure 3E), consistent with the effect of FoxA2 but not FoxA1 on HIF-dependent transcriptional activity (data not shown). Importantly, endogenous FoxA2 was coprecipitated with endogenous HIF-1α (Figure 3F) or HIF-1β (Figure 3G) in TRAMP-C cells maintained under hypoxia. The association of HIF-1β with FoxA2 was abolished following HIF-1α knockdown (Figure 3G), indicating that HIF-1α recruits FoxA2 to the HIF complex under hypoxia. Furthermore, in vitro binding between purified His-FoxA2 and in vitro translated Flag-HIF-1α confirmed their direct interaction (Figure 3H).

Figure 2. Metastasis in *TRAMP*^{Tg}*/Siah2* Mice

(A) H&E staining of indicated tissues from *TRAMP* mice of indicated *Siah2* genotypes. Metastatic lesions are indicated by arrows.

(B) Expression of NE markers in metastatic lesions of *TRAMP/Siah2*$^{+/-}$ mice revealed by IHC staining with indicated antibodies.

(C) Percentage of metastases in *TRAMP* mice with indicated *Siah* genotypes. Number of mice and tissues examined: N = 32 ($S2^{+/+}$ and $S2^{+/-}$), 16 ($S2^{-/-}$), or 9 ($S1a^{+/-}$:$S2^{-/-}$) for liver and lung, and N = 26 ($S2^{+/+}$ and $S2^{+/-}$), 11 ($S2^{-/-}$), or 6 ($S1a^{+/-}$:$S2^{+/-}$) for lymph nodes. For each case, five serial sections of lung or liver were examined by H&E staining.

(D) TUNEL staining (dark brown signals indicated by arrows) of lung sections from *TRAMP/Siah2*$^{+/-}$ and *TRAMP/Siah2*$^{-/-}$ mice.

(E) IHC staining for PCNA on lung sections derived from *TRAMP/Siah2*$^{+/-}$ and *TRAMP/Siah2*$^{-/-}$ mice.

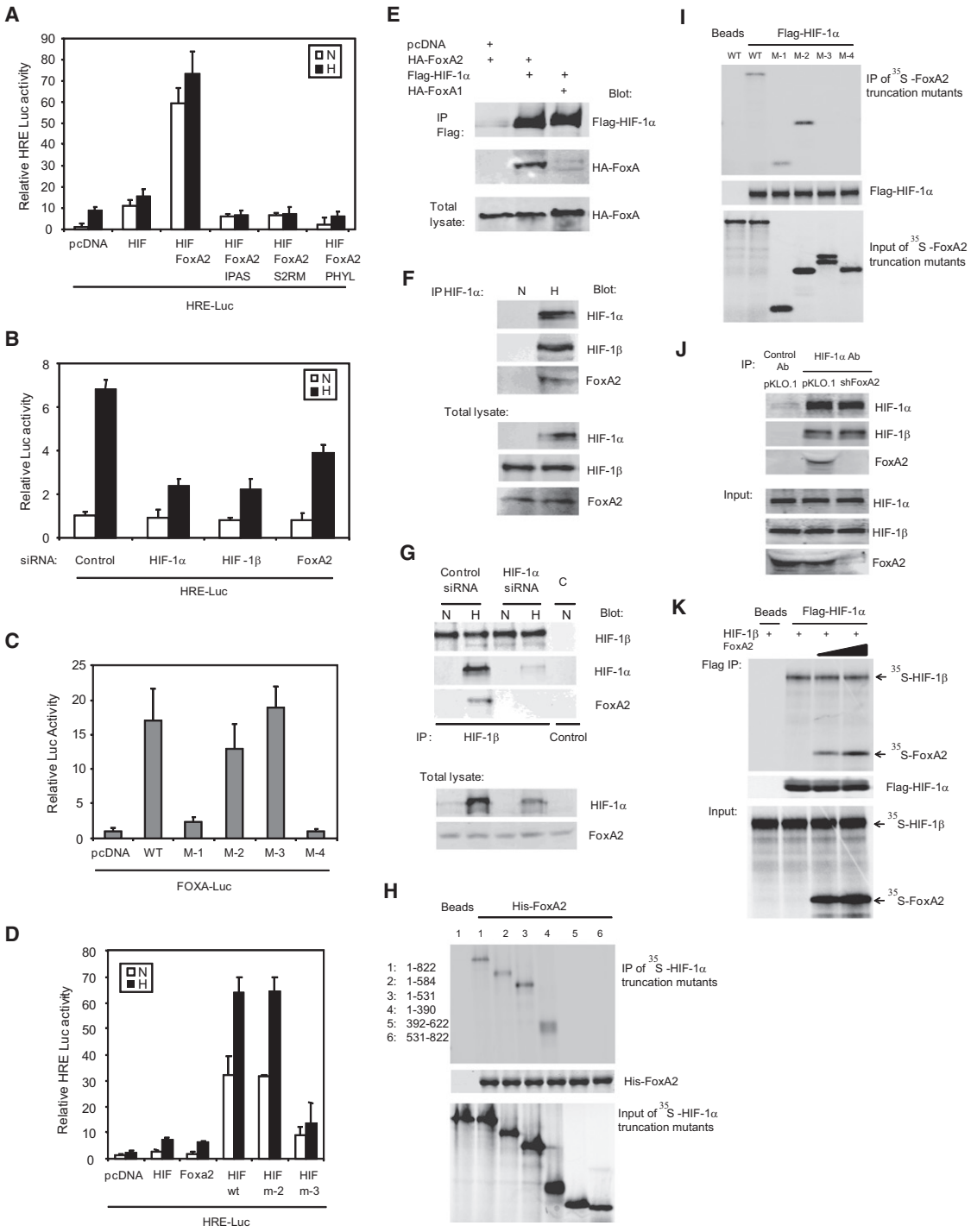

Figure 3. FoxA2 Enhances HIF Transcriptional Activity

(A) TRAMP-C cells were transfected with an HRE-Luc construct and the indicated plasmids. Twenty-four hours after transfection, cells were maintained in 1% oxygen for 10 hr, and cell lysates were collected to measure luciferase activity. β-Gal plasmid was used to normalize for transfection efficiency. N and H denote normoxia and hypoxia, respectively. $p < 0.01$ pcDNA (N) versus HIF (N), $p < 0.0005$ HIF (N) versus HIF+FoxA2 (N).

(B) TRAMP-C cells were first transfected with indicated siRNAs and then 48 hr later with an HRE-luc construct. Twenty-four hours after the second transfection, cells were maintained in 1% oxygen for 10 hr before analysis of luciferase activity. $p < 0.005$ for control (H) versus HIF-1α (H), HIF-1β (H), or FoxA2 (H).

(C) TRAMP-C cells were transfected with the FOXA-Luc construct and indicated FoxA2 deletion mutants. Twenty-four hours after transfection, cells were treated with 1% oxygen for 10 hr before analysis of luciferase activity. $p < 0.01$ WT versus M-1, $p > 0.1$ WT versus M-2 or M-3.

(D) TRAMP-C cells were transfected with an HRE-Luc construct and the indicated plasmids. Twenty-four hours after transfection, cells were maintained in 1% oxygen for 10 hr before analysis of luciferase activity. $p < 0.001$ HIF+WT (N) versus HIF+m3 (N). Each column in (A–D) represents mean ± SD of three replicates.

In vitro binding using truncation mutants of HIF-1α (Figure S2C) and FoxA2 (Figure S2B) identified the bHLH-PAS domain of HIF-1α (Figure 3H) and the N-TAD of FoxA2 (Figure 3I) as the minimal regions mediating the HIF-1α-FoxA2 interaction. Although the bHLH-PAS domain of HIF-1α was found to interact with FoxA2 and the PAS domain of HIF-1α is known to interact with HIF-1β (Erbel et al., 2003), alternation of the FoxA2 level in vitro or in TRAMP-C cells had no apparent effect on the interaction of HIF-1β with HIF-1α (Figures 3J and 3K).

A Subset of HIF Target Genes Is Cooperatively Regulated by FoxA2/HIF-1α

Transcript levels of the HIF targets *VEGFA* and *Glut-1* were not altered after FoxA2 expression or coexpression of HIF-1α and FoxA2 in TRAMP-C, PC3, and HeLa cells (data not shown) suggesting that FoxA2/HIF-1α cooperation selectively affects HIF-regulated genes. We thus compared gene expression profiles of TRAMP-C cells transfected with pcDNA control vector, or expression vectors encoding FoxA2, HIF-1α, or HIF-1α plus FoxA2. Approximately 140 genes in TRAMP-C cells were upregulated by hypoxia (Table S2). Comparison of genes expressed in each condition identified 47 genes upregulated in the HIF-1α + FoxA2 group under hypoxia, in comparison with the other three groups (Table S3). Of these and other hypoxia-induced genes, we further assessed 30 genes for FoxA2-dependent expression, selected based on prostate- and NE tumor-specific expression. To confirm FoxA2-dependent transcription of this gene set, we monitored changes in their expression in TRAMP-C cells expressing FoxA2 siRNA. qRT-PCR analysis of selected genes identified *Hes6*, *Sox9*, *Jmjd1a*, and *Plod2* among those that displayed FoxA2-dependent transcription under hypoxia (Figure 4A). *Sox9*, *Jmjd1a*, and *Plod2* are known HIF target genes (Amarilio et al., 2007; Beyer et al., 2008; Hofbauer et al., 2003). In contrast, transcription of *Glut-1* and *VEGFA* was not altered after FoxA2 knockdown (Figure 4A). Overall, these results suggest that in TRAMP-C cells FoxA2 cooperates with HIF-1α to regulate a subset of HIF targets under hypoxia.

HIF-1α and FoxA2 Cooperate to Activate Hes6 Transcription

The transcription factor *Hes6* is reportedly highly upregulated in human metastatic prostate cancers with a NE phenotype (Vias et al., 2008). Upregulation of Hes6 transcripts under hypoxia suggests that *Hes6* is a HIF target gene. Indeed, knockdown of HIF-1α reduced hypoxia-induced *Hes6* transcription (Figure 4B). We identified three potential HREs and cloned the corresponding 1.25 kb of the mouse Hes6 promoter region upstream of a luciferase reporter. This construct was activated 2.5-fold by the hypoxia mimic DMOG (Figure S3A) and 1.8-fold by hypoxia (data not shown). Deletion analysis of the *Hes6* promoter revealed that the HRE at −66 bp was required for hypoxia-induced reporter activity (Figure S3A). Mutation of this HRE in the full-length 1.25 kb fragment resulted in loss of the response to DMOG (Figure 4C). FoxA2 knockdown repressed *Hes6* transcription (Figures 4A and 4B), whereas FoxA2 overexpression increased *Hes6* promoter activity after addition of DMOG, an effect not seen using the HRE mutant promoter construct (Figure 4D). These observations strongly suggest that FoxA2-induced *Hes6* promoter activity requires an HRE and thus HIF activity. Chromatin immunoprecipitation (ChIP) confirmed that HIF-1α and HIF-1β bound the −66 bp HRE but not the other two putative HREs in the *Hes6* promoter under hypoxia (Figure S3B). ChIP analysis confirmed the binding of FoxA2 to the same −66 bp HRE, which was impaired following HIF-1α knockdown (Figure S3C), suggesting that FoxA2 is recruited to the promoter through HIF-1α. Similarly, FoxA2 bound to HRE-containing promoter regions of *Sox9* (Figure S3C) and *Jmdj1a* (data not shown) in a HIF-1α-dependent manner. These results indicate that FoxA2 regulates a subset of HIF target genes possibly through direct binding to HIF.

FoxA2-Dependent Recruitment of p300 to the Promoters of HIF Target Genes

To analyze mechanisms underlying selectivity of FoxA2 cooperation with HIF-1α, we investigated whether FoxA2 expression changed HIF-1α levels, its asparagine hydroxylation, or its binding to the *Hes6* promoter but found none (data not shown). To directly assess the contribution of FoxA binding sites to FoxA2/HIF-1α cooperation, we determined possible changes in FoxA2/HIF-1α-mediated transactivation using Hes6 promoter mutants (Figure S3D). While a single FoxA site was sufficient to retain full responsiveness to FoxA2/HIF-1α cooperation, a mutation within this element attenuated such cooperation (Figure S3D). Notably, analysis of the effect of FoxA2 on recruitment of p300, a coactivator of HIF transcriptional activity (Arany et al., 1996), revealed that binding of p300 to the *Hes6* promoter was attenuated after FoxA2 knockdown (Figure 4E). FoxA2 knockdown also reduced the binding of p300 to HRE-containing

(E) 293T cells were transfected with indicated plasmids. HIF-1α was precipitated with Flag antibody-conjugated beads (M2) 48 hr posttransfection and the precipitated proteins were analyzed by immunoblotting.
(F) TRAMP-C cells were maintained in 1% O_2 for 5 hr. Endogenous HIF-1α was precipitated and coprecipitated proteins were analyzed by immunoblotting.
(G) TRAMP-C cells were transfected with HIF-1α siRNA for 48 hr then maintained in hypoxia for 5 hr. Endogenous HIF-1β was precipitated and coprecipitated proteins were analyzed by immunoblotting.
(H) HIF-1α and its truncation mutants were translated in vitro, labeled with ^{35}S, and incubated with nickel beads coated with His-FoxA2. After three washes, proteins on the beads were separated by SDS-PAGE and transferred to nitrocellulose membrane. ^{35}S-labeled HIF-1α was detected by phosphor-imager and then immunoblotted with a His antibody to detect His-FoxA2. Four percent of in vitro translated ^{35}S-HIF-1α was used as input.
(I) Flag-HIF-1α was translated in vitro and bound to the M2 beads then incubated with ^{35}S-labeled in vitro translated FoxA2 or its truncation mutants. Bound proteins were monitored as indicated in (H).
(J) TRAMP-C cells were stably transfected with indicated vectors and then grown in 1% O_2 for 6 hr before immunoprecipitation of HIF-1α. The coprecipitated proteins were analyzed by western blotting.
(K) Flag-HIF-1α was translated in vitro and bound to the M2 beads then incubated with ^{35}S-labeled in vitro translated FoxA2 and HIF-1β. Bound proteins were monitored as indicated in (H). See also Figure S2.

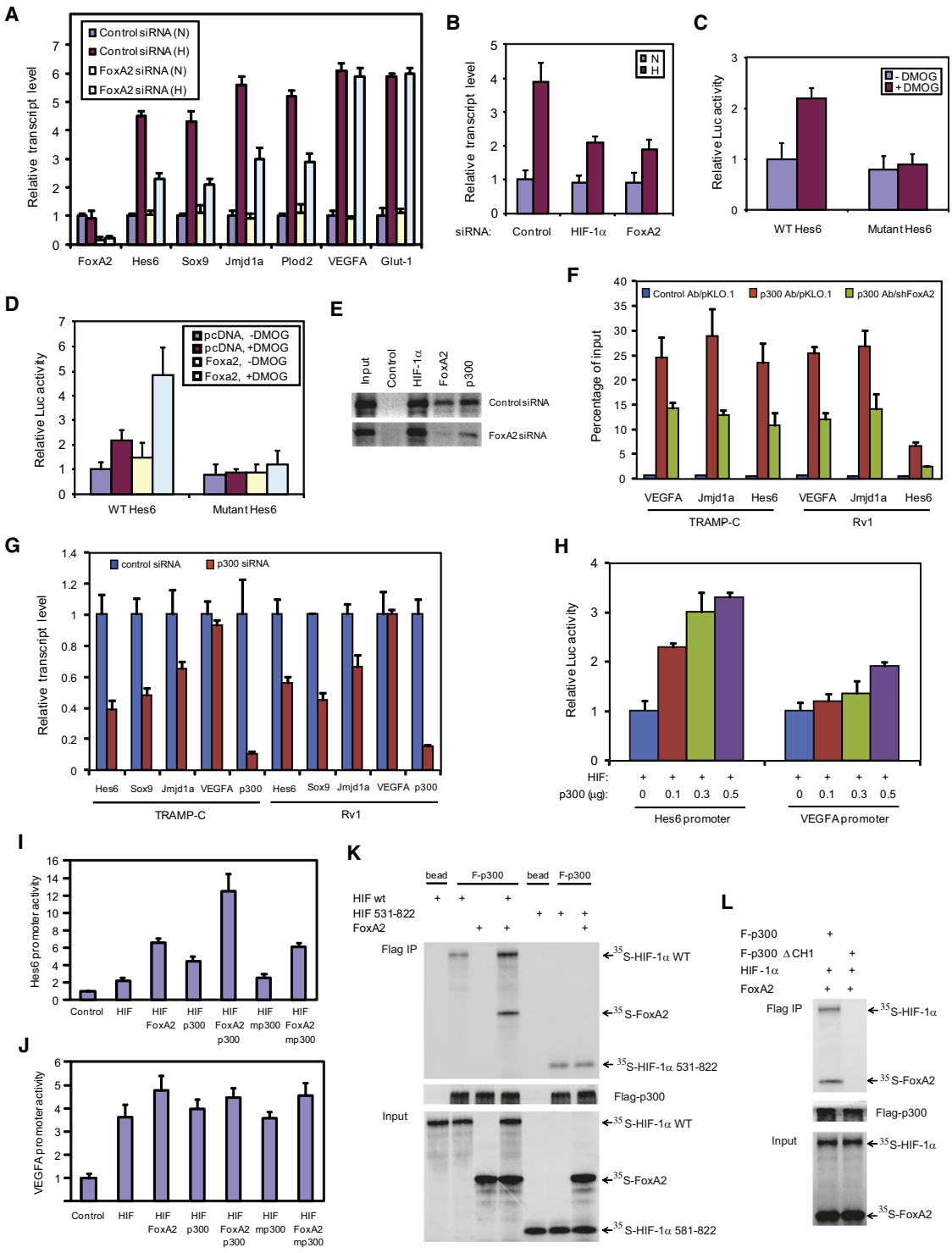

Figure 4. A Subset of HIF Target Genes Are Regulated by Cooperation with FoxA2

(A) TRAMP-C cells were transfected with FoxA2 siRNAs. Forty-eight hours after transfection, cells were maintained in 1% oxygen for 10 hr and then RNA was isolated for qRT-PCR analyses of the indicated transcripts. Control (H) versus FoxA2 (H): $p > 0.1$ for *VEGFA* and *Glut-1*, $p < 0.005$ for all others.

(B) TRAMP-C cells were transfected with indicated siRNAs. Forty-eight hours after transfection, cells were maintained in 1% oxygen for 10 hr. RNA was isolated for qRT-PCR analyses of the *Hes6* transcript. $p < 0.05$ between control (H) and HIF-1α (H), or FoxA2 (H).

(C) TRAMP-C cells were transfected with a 1.25 kb *Hes6* promoter-Luc construct containing the wild-type or mutated −66 bp HRE. Twenty-four hours after transfection, cells were treated with DMOG (1 mM, 16 hr) before analysis of luciferase activity. $p < 0.005$ for WT Hes6 –DMOG versus +DMOG, $p > 0.1$ for mutant Hes6 –DMOG versus +DMOG.

promoters of *Jmjd1a* and *VEGFA* in both TRAMP-C cells and Rv1 cells (Figure 4F). However, p300 knockdown only reduced the transcript levels of *Hes6* and *Jmjd1a* but not *VEGFA* (Figure 4G), which resembled changes seen upon knockdown of FoxA2 (Figure 4A) on the hypoxia-induced transcription of these genes. These results suggest that p300 serves a distinct FoxA2-dependent HIF transcriptional program. Consistent with this possibility, HIF-induced promoter activity of *Hes6* was more sensitive to increased p300 levels than that of *VEGFA* (Figure 4H). Notably, p300, but not p300ΔCH1 (a p300 mutant that cannot interact with HIF-1α), could further increase the degree of HIF/FoxA2 effect on *Hes6* promoter activity (Figure 4I). In contrast, FoxA2 and p300 showed no apparent effect on HIF-dependent activation of the *VEGFA* promoter (Figure 4J). These results suggest that recruitment of p300 is, in part, responsible for the degree and the selectivity of the transcriptional program elicited by HIF/FoxA2 cooperation.

In vitro protein binding showed that FoxA2 enhanced HIF-1α/p300 interaction but had no effect on p300 binding to the HIF-1α 531-822 mutant that cannot associate with FoxA2 (Figure S2C and Figures 3H and 4K). p300 lacking the CH1 domain neither interacted with the HIF/FoxA2 complex (Figure 4L) nor enhanced *Hes6* transcription by HIF/FoxA2 (Figure 4I). These results suggest that FoxA2 promotes HIF and p300 interaction unlikely require HIF-1α N-TAD and p300 CH3 domain (Ruas et al., 2010).

Genes Regulated by HIF/FoxA2 Are Important for Tumorigenesis of TRAMP-C Cells

To determine whether genes regulated by HIF/FoxA2 cooperation are important for tumorigenesis, we employed retroviral vectors to re-express Hes6, Sox9, and Jmjd1a individually or in combination in TRAMP-C cells stably expressing PHYL or FoxA2 shRNA. While the endogenous expression of these genes was attenuated upon expression of PHYL peptide or FoxA2 shRNA, their transcript levels were restored following ectopic expression (Figures S4A and S4B). TRAMP-C cells expressing control pBabe vector or NxN, a mutant PHYL that cannot interact with Siah, but not those expressing PHYL or shFoxA2 could form colonies on soft agar (Figures 5A and 5B). Significantly, coexpression of Hes6, Sox9, and Jmjd1a effectively rescued the ability of TRAMP-C cells expressing either PHYL or shFoxA2 to form colonies in soft agar but reexpression of each individually was insufficient (Figures 5A and 5B). Consistent with the effect of PHYL being Siah dependent, reduction of Siah1a and Siah2 (Figure S4C) reduced levels of HIF-1α protein (Figure S4D) and *Hes6*, *Sox9*, and *Jmjd1a* transcripts (Figure S4E), and attenuated the ability of these cells to form colonies in soft agar under hypoxia (Figure S4F). The reduced ability to form colonies in soft agar could be partially rescued upon re-expression of Hes6, Sox9, and Jmjd1a (Figure S5F).

Similar to the findings in culture, control but not the PHYL-expressing TRAMP-C cells were able to form tumors upon injection into the prostate of mice (Figures 5C–5E). Whereas re-expression of Hes6, Sox9, or Jmjd1a individually in PHYL-expressing TRAMP-C cells failed to rescue tumorigenesis, expression of all three was able to restore tumorigenicity (four of five mice) and partially rescue tumor growth (30% of tumor size) (Figures 5C–5E). Orthotopic injection of shFoxA2-expressing TRAMP-C cells into the prostate also showed significant reduction in tumor formation, which was almost fully rescued by coexpression of Hes6, Sox9, and Jmjd1a (Figures 5F and 5G). These results further establish the importance of HIF/FoxA2 target genes, Hes6, Sox9, and Jmjd1a, in the development of NE prostate tumor.

Genes Coregulated by HIF and FoxA2 Are Important for Hypoxia-Associated NE Phenotype and Metastasis of Human Prostate Adenocarcinoma Cells

We next assessed the importance of the pathway discovered using the *TRAMP* model in human PCa. To this end, we selected CWR22Rv1 cells (Rv1), which were derived from a human prostate adenocarcinoma xenograft displaying an NE phenotype (Huss et al., 2004; Sramkoski et al., 1999). Rv1 cells grown under hypoxia showed upregulation of NE markers NSE and chromogranin B (ChgB) (Figures 6A and 6B) and demonstrated protrusion of neurite-like structures from cells located at the periphery of colonies (Figure 6C). Concomitant with the induction of NE

(D) TRAMP-C cells were transfected with indicated plasmids. Twenty-four hours after transfection, cells were treated with DMOG (1 mM, 16 hr) before analysis of luciferase activity. WT Hes6: $p < 0.01$ pcDNA-DMGO versus pcDNA+DMOG, $p < 0.05$ pcDNA+DMGO versus Foxa2+DMOG.

(E) TRAMP-C cells were transfected with control or FoxA2 siRNA. Forty-eight hours after transfection, cells were grown in 1% oxygen for 5 hr before ChIP assays of the HRE-containing region of *Hes6* promoter were performed using indicated antibodies. PCR products were analyzed on 2% agarose gel electrophoresis. A representative reversed gel image of triplicate experiments is shown.

(F) FoxA2 shRNA-expressing cells were treated with 1% oxygen for 6 hr and subjected to ChIP assays with p300 antibodies. The immunoprecipitated materials were used for QPCR analyses of the HRE-containing regions of *VEGFA*, *Jmjd1a*, and *Hes6*. The results of ChIP QPCR were normalized to those of the input. $p < 0.01$ for all genes between control and shFoxA2 for both cell lines.

(G) Cells were transfected with control or p300 siRNA for 48 hr and then analyzed by qRT-PCR for the indicated transcripts. Both TRAMP-C and Rv1: $p > 0.1$ control versus p300 siRNA for *VEGFA* and $p < 0.05$ for all others.

(H) TRAMP-C cells were cotransfected with *Hes6* or *VEGFA* promoter-Luc vector, HIF-1α, and increasing amounts of p300. Twenty-four hours after transfection, cell lysates were collected for a luciferase assay. Hes6: $p < 0.001$ 0 μg versus all three; VEGFA: $p < 0.005$ 0 μg versus 0.5 μg, $p > 0.1$ 0 μg versus the other two.

(I and J) TRAMP-C cells were transfected with *Hes6* promoter-Luc (I) or *VEGFA* promoter-Luc (J) together with the plasmids indicated. Twenty-four hours after transfection, cell lysates were collected for analysis of luciferase activity. Hes6: $p < 0.01$ HIF versus HIF+FoxA2, HIF versus HIF+p300, and HIF+FoxA2 versus HIF+FoxA2+p300; VEGFA: $p > 0.1$ for these comparisons. In (A)–(D) and (F)–(J), each column represents mean ± SD of three experiments.

(K) Flag-p300 was translated in vitro and coupled to M2 beads. HIF-1α or FoxA2 was translated in vitro and labeled with ^{35}S. Equal amounts of ^{35}S-HIF-1α and ^{35}S-FoxA2 were incubated with M2 bead-bound Flag-p300. Bound proteins were monitored as indicated in Figure 3H.

(L) Flag-p300 (wt or ΔCH1) was translated in vitro and bound to M2 beads. HIF-1α and FoxA2 were translated in vitro and labeled with ^{35}S. Equal amount of ^{35}S-HIF-1α and ^{35}S-FoxA2 was mixed and incubated with M2 bead-bound Flag-p300 or Flag-p300ΔCH1. Bound proteins were monitored as indicated in Figure 3H. See also Figure S3 and Tables S2 and S3.

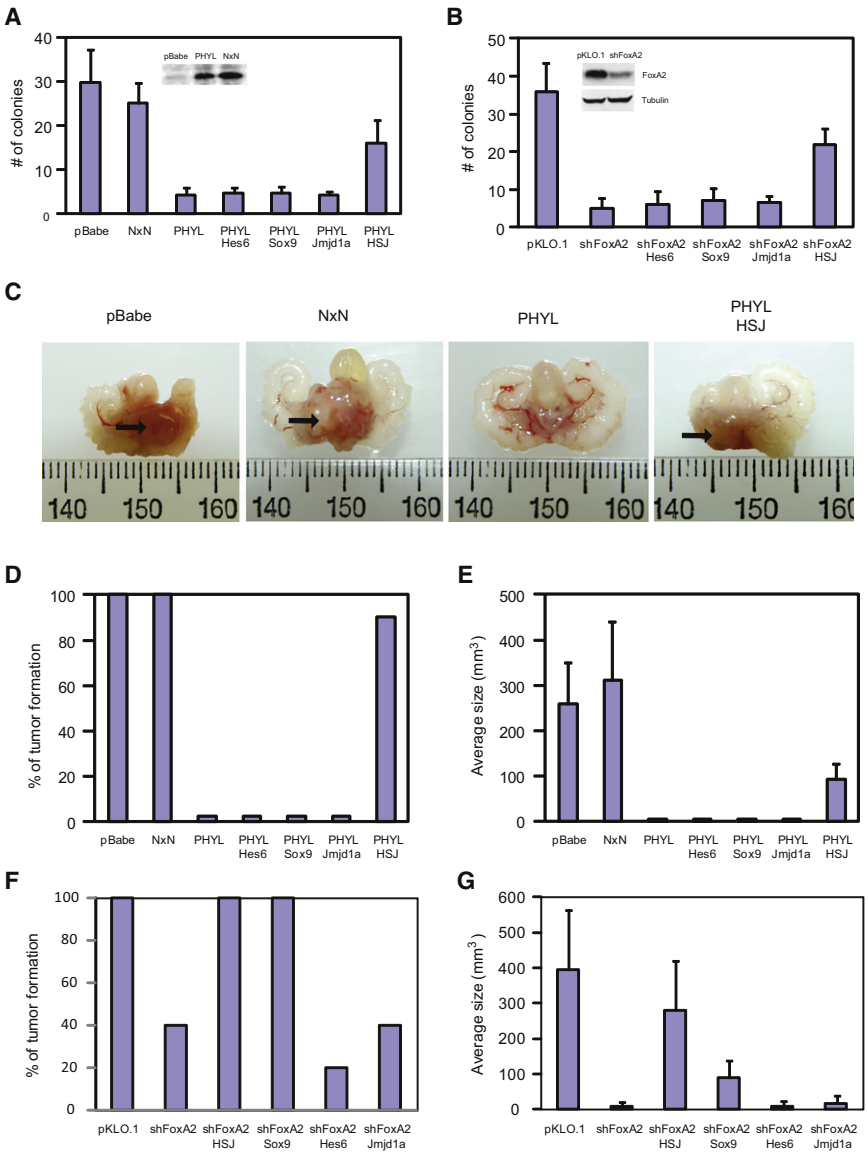

Figure 5. Hes6, Sox9, and Jmjd1a Are Required for Tumorigenesis of *TRAMP* Cells

(A) TRAMP-C cells were stably transfected with indicated vectors. The inset shows a western blot of PHYL and NxN. PHYL-expressing cells were then infected with retroviral constructs encoding Hes6, Sox9, or Jmjd1a individually or all together (HSJ). Cells (1×10^5) were monitored for growth on soft agar under 1% O_2 for 3 weeks. Shown is the number of colonies per well of six-well plate. $p = 0.4$ (pBabe versus NxN), $p = 0.053$ (NxN versus PHYL+HSJ), $p < 0.0005$ (NxN versus PHYL, PHYL+Hes6, PHYL+Sox9, or PHYL+Jmjd1a), $p < 0.05$ (PHYL+HSJ versus PHYL, PHYL+Hes6, PHYL+Sox9, or PHYL+Jmjd1a).

(B) TRAMP-C cells were transfected with indicated shRNA. The inset shows a western blot of FoxA2. shFoxA2-expressing cells were then infected with retroviral constructs of Hes6, Sox9, or Jmjd1a individually or all together (HSJ). Cells (1×10^5) were monitored for their growth on soft agar under 1% O_2 for 3 weeks. Shown is the number of colonies per well of six-well plate. $p = 0.06$ (pKLO.1 versus shFoxA2+HSJ), $p < 0.005$ (pKLO.1 versus shFoxA2, shFoxA2+Hes6, shFoxA2+Sox9, or shFoxA2+Jmjd1a), $p < 0.005$ (shFoxA2+HSJ versus shFoxA2, shFoxA2+Hes6, shFoxA2+Sox9, or shFoxA2+Jmjd1a). In (A) and (B), each column represents mean ± SD for three replicates.

(C–G) TRAMP-C transfectants (1×10^6) as described in (A) and (B) were injected into the prostate of nude mice. Two months after injection, genitourinary tracts of mice were dissected and prostate tumor formation was quantified. (C) shows the representative images of prostate tumors, which were indicated by arrows. (D) and (F) depict the frequency of tumor formation. (E) and (G) show the average size of the tumors formed. In (E) and (G), each column represents mean ± SD for five mice. $p < 0.05$ pBabe versus PHYL+HSJ and NxN versus PHYL+HSJ, $p < 0.001$ (pKLO.1 versus shFoxA2, shFoxA2+Hes6, or shFoxA2+Jmjd1a), $p < 0.005$ (shFoxA2+HSJ versus shFoxA2, shFoxA2+Hes6, or shFoxA2+Jmjd1a), $p < 0.01$ (pKLO.1 versus shFoxA2+Sox9), $p = 0.2$ (pKLO.1 versus shFoxA2+HSJ). See also Figure S4.

phenotype was the upregulation of *Hes6*, *Sox9*, and *Jmjd1a* transcripts (Figure 6D). Significantly, inhibition of Siah or knockdown of FoxA2 attenuated hypoxia-induced upregulation of *Hes6*, *Sox9*, and *Jmjd1a* (Figures S5A and S5B). To determine whether *Hes6*, *Sox9*, and *Jmjd1a* are important for hypoxia-induced NE phenotype, we re-expressed these genes individually or in combination in PHYL- or shFoxA-expressing Rv1 cells (Figures S5A and S5B) and found only coexpression of all three could partially restore hypoxia-induced NSE upregulation and formation of neurite-like structures (Figures 6E–6G). These results point to a requirement for Siah-HIF/FoxA2-regulated genes in the hypoxia-induced NE phenotype of human prostate adenocarcinoma cells.

To evaluate the biological significance of NE phenotype for human prostate cancer in vivo, we injected the above Rv1 transfectants into the prostate of nude mice. Surprisingly, unlike TRAMP-C cells, Rv1 cells expressing PHYL only showed about 30% reduction in the tumor size which could not be rescued by coexpression of Hes6, Sox9, and Jmjd1a (Figure 6H). Similarly, Rv1 cells expressing shFoxA2 did not exhibit any notable decrease in tumor formation (Figure 6H). These results indicate that Hes6, Sox9, and Jmjd1a are not involved in tumorigenesis of Rv1 cells. The 30% reduction of tumor size by PHYL was correlated with a 35% reduction in the tumor vessel density (Figure S5C and Table S4) and 40% reduction of *VEGFA* transcript in PHYL-expressing Rv1 cells in vitro (Figure S5D). Similarly, colony formation in the soft agar assay was comparable for PHYL-expressing Rv1 cells and control cells (Figure S5E). Significantly, the circulating PHYL- or shFoxA2-expressing Rv1 cells in the blood were reduced, indicating impaired intravasation of these cells, which was partially rescued by coexpression of Hes6, Sox9, and Jmjd1a (Figure 6I). Although Rv1 cells

exhibited limited ability to form liver metastasis (two out of ten mice injected with Rv1 cells), they were very efficient in periaortic lymph node metastases. Expression of PHYL or shFoxA2 abolished lymph node metastases of Rv1 cells, which could be largely restored by coexpression of Hes6, Sox9, and Jmjd1a (Figure 6J). These findings suggest that genes coregulated by HIF and FoxA2 play a key role in metastasis of prostate adenocarcinoma cells.

IHC analyses of Rv1 orthotopic tumors revealed that HIF-1α and NSE staining were concentrated around the necrotic regions, which are known to be highly hypoxic, whereas FoxA2 staining was evenly distributed (Figure 6K). As expected, expression of PHYL resulted in reduced HIF-1α staining and loss of NSE staining in the hypoxic regions (Figure 6K). FoxA2 shRNA reduced the NSE staining in the hypoxic regions without affecting HIF-1α levels (Figure 6K), consistent with our in vitro data (Figures 6E–6G). Importantly, consistent with our in vitro results, coexpression of Hes6, Sox9, and Jmjd1a in PHYL- or shFoxA2-expressing Rv1 cells restored the NSE staining in the hypoxic regions (Figure 6K). Strong NSE staining was primarily seen within the more hypoxic regions, proximal to the necrosis, of the primary tumor (Figure 6K) and metastatic lesions in liver and lymph nodes (Figure 6L), implying that the NE-differentiated Rv1 cells may be responsible for the metastasis. These results establish that genes coregulated by HIF and FoxA2 play a key role in hypoxia-induced NE phenotype of PCa in vitro and in vivo, and that NE phenotype is tightly associated with PCa metastasis.

Expression of FoxA2-HIF-1α Target Genes in Prostate Tumors

We next asked whether FoxA2/HIF-1α transcriptional targets were expressed in NE tumors. The very few NE tumors identified in a *TRAMP/Siah2*$^{-/-}$ mice had lower transcript levels of *Hes6*, *Sox9*, *Jmjd1a*, and *Plod2* compared with *TRAMP/Siah2*$^{+/-}$-derived NE tumors (Figure 7A), consistent with HIF-1α-dependent expression.

The NE phenotype seen in human PCa can be classified to three types based on IHC staining of NE markers (Cindolo et al., 2007; Hirano et al., 2005; Shimizu et al., 2007): focal, in which NE markers distinguish clusters of cells, found in low-grade and moderately differentiated PCa; general staining, in which larger tumor areas are positive for NE markers, found in high-grade and poorly differentiated PCa; and single cells that are stained positively for NE markers (Hirano et al., 2005). We examined 15 cases of human PCa and found 10 to exhibit NE phenotype. Two of the 10 samples displayed focal staining of NE marker NSE, where FoxA2, Hes6, and Sox9 were concentrated in the NE foci (Figure 7B and Figure S6A). Eight of the ten specimens showed a general staining of NSE, with costaining of FoxA2, Hes6, and Sox9 in five of eight cases. Coexpression of FoxA2, Hes6, and Sox9 found in 70% of PCa specimens with NE phenotype was statistically significant ($p < 0.05$; Figure 7C).

We next performed IHC staining of a human prostate TMA consisting of 79 cases representing prostatic intraepithelial neoplasia (PIN) and different Gleason stages of PCa. A higher NSE staining was found in high-grade PCa (G4 and G5), which also showed increased staining of Siah2, FoxA2, Hes6, and Sox9, compared with low-grade tumors (PIN and G3) (Figure 7D). The difference in the expression of NSE, Siah2, FoxA2, Hes6, and Sox9 between high-grade and low-grade tumors is statistically significant and correlated with pathoclinical staging. In addition, IHC staining of three human prostate NE tumors revealed coexpression of synaptophysin, FoxA2, HIF-1α, Hes6, and Sox9 in all cases (Figure S6B). These findings suggest that NE-positive tumors are associated with the more malignant human prostate cancers, in which the HIF/FoxA2 target genes are expected to play a role in the development of the NE phenotype. In agreement, gene expression data from human prostate adenocarcinoma identified a marked increase in *Hes6*, *Plod2*, *Jmjd1a*, and *FoxA2* expression in metastatic prostate tumors, compared with primary prostate tumors and normal prostate tissues (Figure 7E). The expression of these genes correlates with the expression of NE markers, further illustrating the link between their expression, NED, and metastatic prostate tumors (Figure 7E).

Whereas Siah2 staining was higher in high-grade PCa, HIF-1α staining was found in both low-grade and high-grade tumors (Figure 7D). Despite high level of HIF-1α expression in all grades of tumors, the level of Glut-1, a common readout for HIF transcriptional activity, was high only in high-grade PCa, pointing to a correlation between Siah2 expression and HIF-1α activity (Figure 7D). In agreement, gene expression analyses revealed an increased *Siah2* transcript and enhanced HIF activity in metastatic PCa as reflected by increased transcript of HIF target genes such as *CA9*, *VEGFA*, and *Glut-1*, compared with primary PCa (Figure 7E). These results substantiate the correlation between Siah2 expression and HIF activity in human PCa, consistent with the role of Siah in regulation of PHD3 and factor-inhibiting HIF-1 (FIH) stability, which control HIF-1α availability and activity (Nakayama et al., 2004; Fukuba et al., 2008). The cooperation between HIF and FoxA2 in determining NE phenotype can be attributed to a higher level of Siah2 which increases HIF stability and activity, and availability of FoxA2 in the high-grade PCa.

DISCUSSION

Our results provide insight into regulation and function of the FoxA2/HIF-1α complex in determining NE prostate tumor formation and NE phenotype, an important component of metastatic prostate adenocarcinomas. These results also point to a role for Siah2 in determining tumor differentiation. Siah2 loss has little effect on development and growth of the prostate luminal epithelium but decreases initiation of NE carcinomas and, consequently, the metastatic burden in the *TRAMP* model. We show that partial deletion of *Siah1a* on a *Siah2* null background fully ablated NE tumor formation, suggesting that both Siah2 and Siah1 are required to enable the development of prostate NE tumors.

As HIF-1α is stabilized under hypoxia and FoxA2 is expressed in NE tissues, our findings suggest conditional and spatial cooperation between these two factors under specific tissue and oxygen requirements. Siah2-dependent regulation of HIF coupled with NE-specific expression of FoxA2 provides a framework for a specific tumor differentiation program associated with a highly metastatic phenotype. Among the

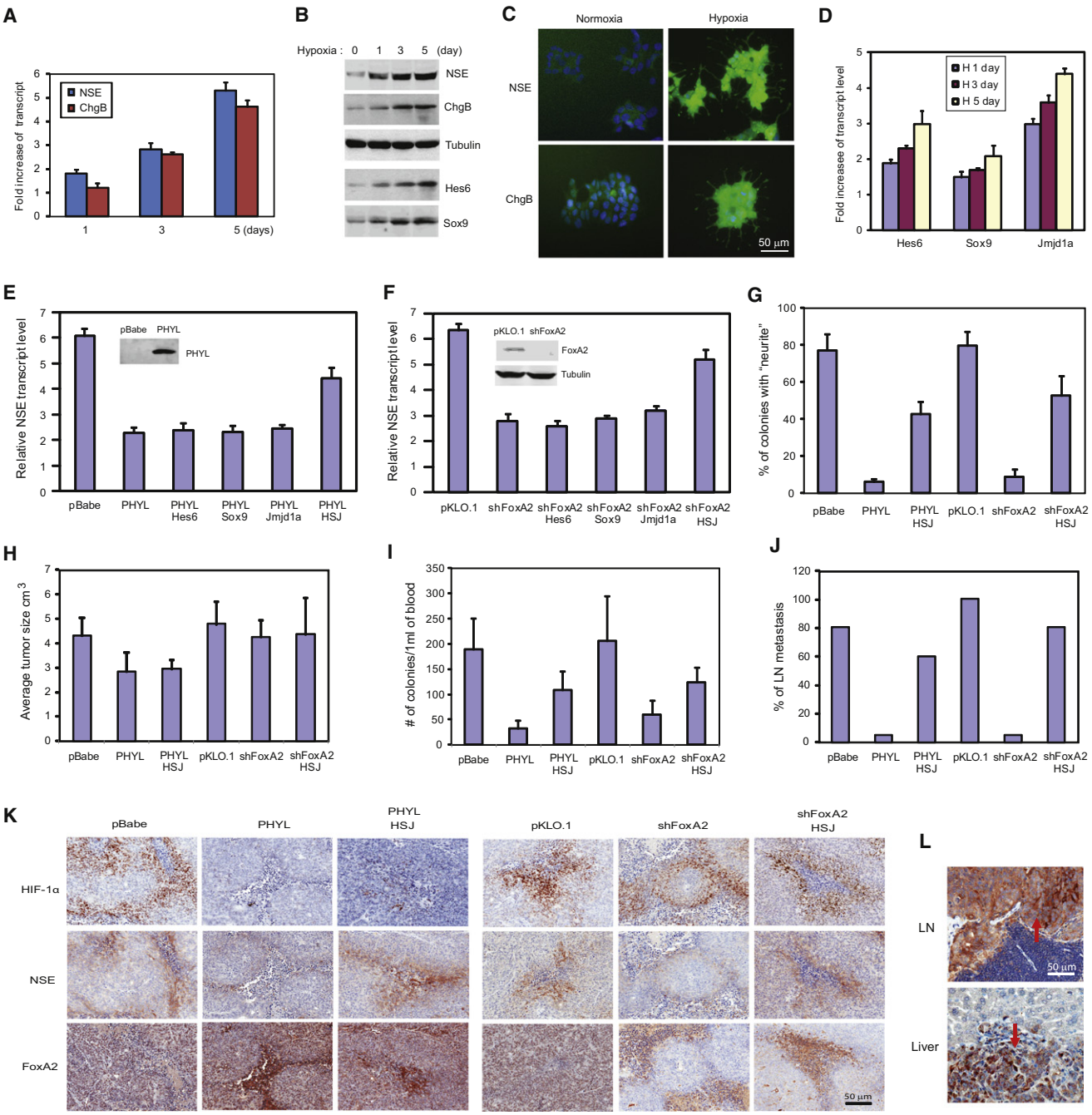

Figure 6. Hypoxia-Induced NE Phenotype in Human Prostate Cancer Cells

(A) CWR22Rv1 cells were cultured under normoxia or hypoxia (1% O_2) for indicated times before qRT-PCR analysis of *NSE* and *ChgB*. Transcript levels under hypoxia were normalized to those under normoxia. $p < 0.05$, $p < 0.005$, $p < 0.0001$ for *NSE* hypoxia versus normoxia at days 1, 3, and 5, respectively. $p = 0.19$, $p < 0.005$, $p < 0.0001$ for *ChgB* hypoxia versus normoxia at days 1, 3, and 5, respectively.

(B) Rv1 cells were grown under 1% O_2 for indicated times. The total lysates were used for western blot analyses of NSE and ChgB. Hes6 and Sox9 were immunoprecipitated followed by western blot analysis.

(C) Rv1 cells were seeded onto the tissue culture plate at low density and cultured in 1% O_2 for 6 days. Cells were fixed and immunostaind for NSE or ChgB. Note the neurite-like protrusions from cells cultured under hypoxia.

(D) Rv1 cells were cultured under hypoxia for indicated times before qRT-PCR analysis. The transcript level under hypoxia was normalized to that of corresponding normoxia samples. $p < 0.005$ for all three transcripts at all three time points.

(E) Rv1 cells were stably transfected with control pBabe vector or PHYL. In the inset, a western blot shows expression of PHYL. PHYL-expressing Rv1 cells were further infected with viral constructs of Hes6, Sox9, or Jmjd1a either individually or in combination (HSJ). Cells were cultured under 1% O_2 for 5 days before qRT-PCR analysis of NSE. $p < 0.01$ pBabe versus PHYL+HSJ, $p < 0.0001$ pBabe versus all others, $p < 0.005$ PHYL+HSJ versus other PHYL-expressing cells.

four FoxA2/HIF targets identified in this study, Hes6 is reportedly highly upregulated in metastatic prostate cancers displaying NE markers (Vias et al., 2008) and Plod2 is overexpressed in metastatic prostate NE tumors (Shah et al., 2004). Sox9 expression is increased in relapsed androgen-refractory prostate cancers and is associated with enhanced growth, invasion and angiogenesis (Wang et al., 2008). It is noteworthy that Hes6, Sox9, and Jmjd1a have been shown to regulate differentiation of stem/progenitor cells (Eun et al., 2008; Loh et al., 2007; Nowak et al., 2008), raising the possibility that FoxA2/HIF cooperation initiates a transcriptional program that regulates neuroendocrine differentiation of normal and/or prostate cancer stem cells. In agreement, the NE phenotype of PCa is also associated with expression of the stem/progenitor markers, supporting the notion that the NE-like cells may harbor prostate cancer stem cells (Bonkhoff, 1998; Sotomayor et al., 2009).

Several plausible mechanisms could underlie HIF-1α/FoxA2 transcriptional synergy; we ruled out that the intrinsic chromatin remodeling activity of FoxA2 is important (Cirillo et al., 2002) and that FoxA2 displaces HIF-1β. Our data implicate FoxA2 in enhanced recruitment of p300 for the selective activation of a subset of HIF-target genes. Consistent with our findings, MEFs from mice expressing a p300/CBP mutant that cannot interact with HIF exhibited attenuated HIF activity in luciferase reporter assays, but they showed attenuated expression of only a small subset of HIF target genes, not including *VEGFA* and *Glut-1* (Kasper et al., 2005).

The importance of *Hes6*, *Sox9*, and *Jmjd1a* for NE phenotype is demonstrated in human PCa cells that exhibit NE phenotype under hypoxia. Inhibition of these genes attenuates the NE phenotype and PCa metastasis, whereas their coexpression rescues the NE phenotype and metastasis even upon knockdown of FoxA2 or Siah2, their upstream regulators. Notably, the requirement of hypoxia for NE phenotype was confirmed by IHC analyses of PCa in vivo where level of NSE coincided with that of HIF, FoxA2, and their regulated genes. Of equal significance, inhibition of mouse prostate tumor growth by attenuating Siah2 activity could be overcome upon coexpression of Hes6, Sox9, and Jmjd1a, further illustrating the importance of their cooperation for prostate tumor development.

Overall, our study offers a paradigm underlying formation of NE phenotype and NE prostate tumor development. This pathway requires the ubiquitin ligase Siah2, which determines the level and activity of HIF-1α, which then cooperates with the NE-specific transcription factor FoxA2. It is the conditional and spatial regulation of these factors that transactivates a subset of genes critical for NE phenotype and metastasis of PCa as well as for development of NE prostate tumors. Common to NE prostate tumors and PCa harboring the NE phenotype is their strong propensity to metastasize, and the poor outcome associated with these more aggressive forms of prostate cancer. Our findings unveil mechanisms underlying their development and progression, respectively, while identifying possible targets for therapy and markers for improved detection and monitoring of these tumors.

EXPERIMENTAL PROCEDURES

Prostate Tumor Samples

Prostate tumor samples representing NE tumors and/or prostate adenocarcinomas were obtained as part of approved clinical studies from the University of California Davis (IRB #200312072), University of California Irvine (SPECS project, IRB #20005-4806), and Northwestern University (SPORE tissue banking protocol, IRB #NCI01X2: STU00009126). In all cases, informed consent was obtained from all subjects.

Animal Studies

All animals were housed in the Sanford-Burnham Institute's animal facility and the experiments with live animals were approved by our institute animal committee (IACUC #04-135, 04-141, 07-132) and conducted following the institute's animal policy in accordance with NIH guidelines.

Cell Lines

TRAMP-C cells were maintained in Dulbecco's modified Eagle's medium (DMEM) supplemented with 5% Nu-serum IV, 5% fetal bovine serum (FBS), 5 μg/ml insulin, and antibiotics. CWR22 Rv1 cells were maintained in RPMI1640 medium with 5% FBS and antibiotics.

Generation of *TRAMP* Mice in a *Siah2* Knockout Background

Siah2$^{+/-}$ mice (129 SVJ strain) were crossed with *TRAMP* transgenic mice (C57/Bl6 strain) to obtain Siah2 heterozygotes carrying the *TRAMP* transgene (C57/Bl6 and 129 SVJ mixed strain). Female *Siah2*$^{+/-}$/*TRAMP* mice were

(F) Rv1 cells were transfected with control pKLO.1 vector or FoxA2 shRNA. In the inset, a western blot shows the knockdown of FoxA2. shFoxA2-expressing cells were further infected with viral constructs of Hes6, Sox9, or Jmjd1a either individually or in combination (HSJ). Cells were cultured under 1% O_2 for 5 days before qRT-PCR analysis of NSE. $p < 0.05$ pKLO.1 versus shFoxA2+HSJ, $p < 0.0001$ pKLO.1 versus all others, $p < 0.001$ shFoxA2+HSJ versus other shFoxA2-expressing cells.

(G) Rv1 transfectants were seeded on tissue culture plates at low density and maintained at 1% O_2 for 6 days. The morphology of cells was examined under phase-contrast microscopy. The number of colonies with neurite-like structures (criteria: greater than one-third of cells in the periphery of colonies have neurite-like structure that is >20 μm long) were scored at triplicate of six-well plates. $p < 0.01$ pBabe versus PHYL or PHYL+HSJ, $p < 0.001$ PHYL+HSJ versus PHYL, $p < 0.05$ pKLO.1 versus shFoxA2 or shFoxA2+HSJ, $p < 0.005$ shFoxA2 versus shFoxA2+HSJ. In (A) and (D)–(G), each column represents mean ± SD for three replicates.

(H) Rv1 transfectants (1×10^6) as described in (E) and (F) were injected into the prostates of nude mice. Four weeks after injection, the orthotopic tumors were collected and size measured. $p < 0.05$ pBabe versus PHYL or PHYL+HSJ, $p > 0.1$ PHYL versus PHYL+HSJ and pKLO.1 versus shFoxA2 or shFoxA2+HSJ.

(I) Blood was collected from the heart of mice described in (H) before the sacrifice, cultured in the selection medium for 2 weeks. The number of colonies on the plates was scored and normalized to the volume of blood. $p < 0.01$ pBabe versus PHYL or PHYL+HSJ, $p < 0.001$ PHYL versus PHYL+HSJ, $p < 0.05$ pKLO.1 versus shFoxA2 or shFoxA2+HSJ, $p < 0.005$ shFoxA2 versus shFoxA2+HSJ. In (H) and (I), each column represents mean ± SD for five mice.

(J) Lymph nodes (LN) were collected from the mice described in (H) and stained with H&E so that the metastases could be determined. $p < 0.05$ (pBabe versus PHYL), $p = 0.17$ (PHYL versus PHYL+HSJ), $p < 0.01$ (pKLO.I versus shFoxA2), $p < 0.05$ (shFoxA2 versus shFoxA2+HSJ).

(K) Orthotopic tumor sections as described in (H) were subjected to IHC staining of NSE, HIF-1α, and FoxA2.

(L) The LN or liver metastasis from Rv1 orthotopic model was subjected to IHC staining of NSE. See also Figure S5 and Table S4.

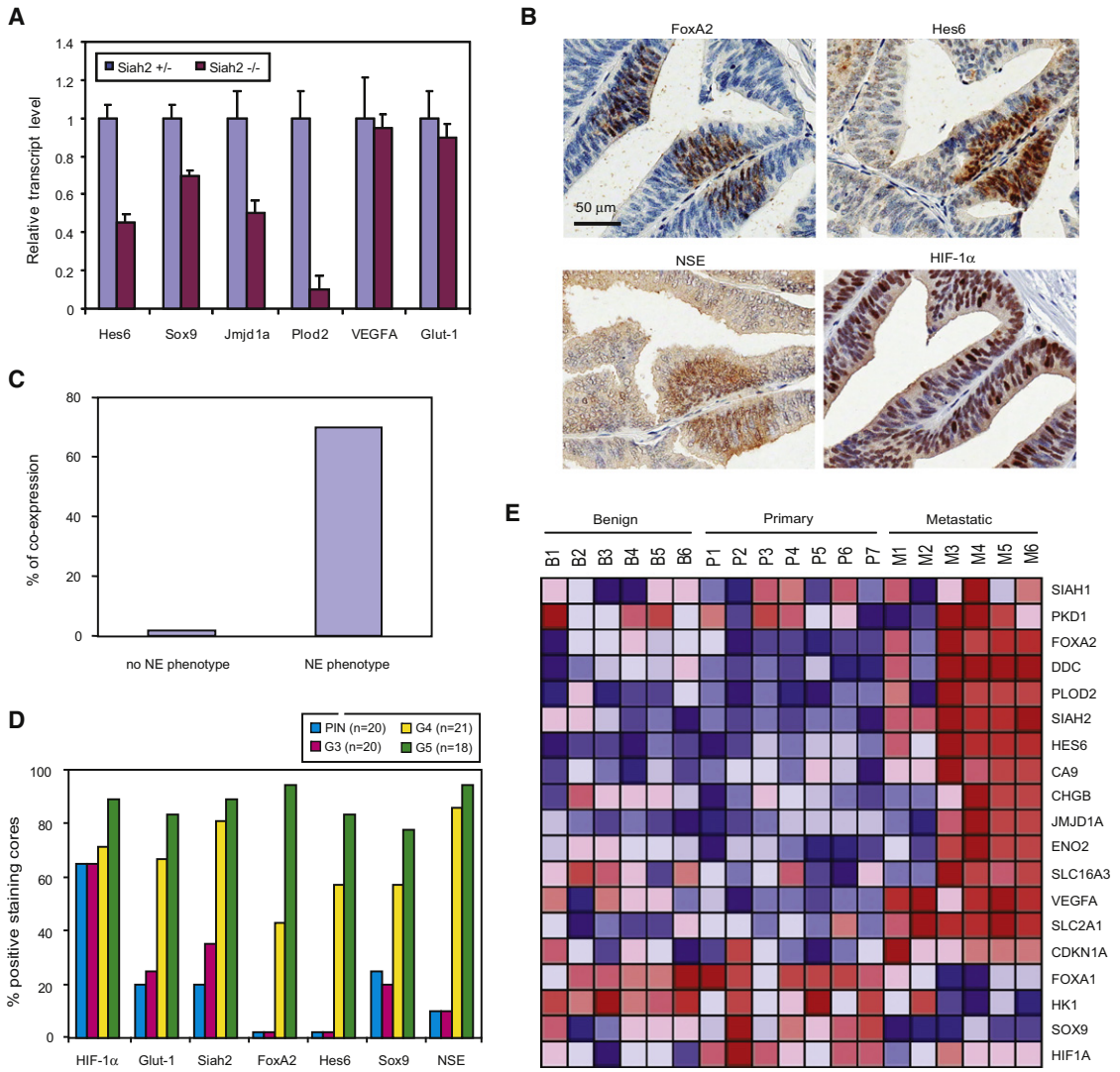

Figure 7. Changes in HIF/FoxA2 Targets in Prostate Tumors

(A) Laser capture microdissection was performed to collect NE carcinoma cells from tumors of *TRAMP/Siah2*$^{+/-}$ or *TRAMP/Siah2*$^{-/-}$ mice. RNA was isolated for qRT-PCR analyses of indicated transcripts. Each column represents mean ± SD for two replicates. *Siah2*$^{+/-}$ *versus Siah2*$^{-/-}$: $p < 0.05$ for *Hes6*, *Sox9*, and *Jmjd1a*, $p = 0.78$ and 0.46 for *VEGFA* and *Glut-1*, respectively.

(B) IHC of FoxA2, Hes6, and HIF-1α was performed on a human prostate adenocarcinoma with NED foci. Shown are representative images with a corresponding NE control marker NSE.

(C) IHC staining using the indicated antibodies was performed on serial sections of 15 human PCa specimens, among which ten cases have NE phenotype (NSE positive) and five cases have no NE phenotype (NSE negative). Coexpression of Hes6, Sox9, and Jmjd1a in human PCa with NE phenotype is statistically significant compared with that in human PCa without NE phenotype ($p < 0.05$).

(D) IHC staining of the indicated proteins was performed on a human prostate TMA consisting of PINs and prostate cancers of various Gleason scores; the numbers of each tumor group are shown on the figure. The staining intensity is scored according to four scales by two pathologists: 0 (no staining), 1 (weak staining), 2 (medium staining), and 3 (strong staining). Scale 0 and 1 are defined as negative staining, and scale 2 and 3 are defined as positive staining. Shown is the percentage of cores that are positively stained for indicated antibodies.

(E) Shown are clustered patterns of gene expression taken from GSE3325. Columns represent tumor samples (Benign, B1-B6; Primary, P1-P7; Metastatic, M1-M6), and rows represent genes. The heatmap represents higher expression levels in red and lower levels in blue. Expression data for each gene were row normalized. Transcript levels of *Siah2*, *FoxA2*, *Hes6*, *Jmjd1a*, *Plod2*, *DDC*, *ChgB*, and *ENO2* in metastatic PCa are statistically significantly higher than those in primary PCa. See also Figure S6.

crossed with male *Siah2*$^{+/-}$ mice to generate male *TRAMP* mice of three genotypes (*Siah2* $^{+/+, +/-, -/-}$), which were predominantly of the 129 strain. Female *Siah2*$^{+/-}$*/TRAMP* mice were also crossed with male *Siah1a*$^{+/-}$*Siah2*$^{+/-}$ mice to generate male *TRAMP* mice with a *Siah1a*$^{+/-}$*Siah2*$^{-/-}$ genotype. *Siah/TRAMP* mice were analyzed at 8 months of age.

Antibodies and Reagents

Antibodies to HIF-1α, HIF-2α, and Sox9 (NOVUS), to Hes6, Jmjd1a, p300, and NSE (Abcam), to synaptophysin (BD Bioscience), to FoxA2, HIF-1β, and CD31, Chromogranin B (Santa Cruz), to active caspase-3, Glut-1 (Chemicon), to PCNA (Cell Signaling), to Siah2, FLAG, HA, α-tubulin, and β-actin (Sigma)

were used according to the manufacturers' recommendations. An ApopTag peroxidase in situ apoptosis kit was obtained from Chemicon.

Statistical Analysis

Student's t test or Fisher's exact test was used for the statistical analyses.

ACCESSION NUMBERS

Microarray data were deposited in the GEO database (GSE18478).

SUPPLEMENTAL INFORMATION

Supplemental Information includes Supplemental Experimental Procedures, six figures, and Tables S1, S2, S3 and S4 and can be found online at doi:10.1016/j.ccr.2010.05.024.

ACKNOWLEDGMENTS

We thank members of the Ronai Lab for helpful discussions. We thank Drs. Lorenz Poellinger, Hueng-Sik Choi, Wei Gu, Andreas Möller, Collin House, Robert Abraham, Gary Chiang, Norman Greenberg, James Jacobberger, Marja Nevalainen, for reagents, Jeremy Mathews for preparation of the prostate tumor TMA, Ling Wang for help with intraprostatic injection, Joan Massague for protocol of retroviral infections. Support by NCI grant CA111515 (to Z.A.R.), P50CA090386 (K.K.), and U01CA114810 (to D.M.) is gratefully acknowledged. J.Q. was supported by a CIHR fellowship.

Received: October 18, 2009
Revised: March 25, 2010
Accepted: May 14, 2010
Published: July 12, 2010

REFERENCES

Ahmed, A.U., Schmidt, R.L., Park, C.H., Reed, N.R., Hesse, S.E., Thomas, C.F., Molina, J.R., Deschamps, C., Yang, P., Aubry, M.C., and Tang, A.H. (2008). Effect of disrupting seven-in-absentia homolog 2 function on lung cancer cell growth. J. Natl. Cancer Inst. *100*, 1606–1629.

Amarilio, R., Viukov, S.V., Sharir, A., Eshkar-Oren, I., Johnson, R.S., and Zelzer, E. (2007). HIF1alpha regulation of Sox9 is necessary to maintain differentiation of hypoxic prechondrogenic cells during early skeletogenesis. Development *134*, 3917–3928.

Aragones, J., Fraisl, P., Baes, M., and Carmeliet, P. (2009). Oxygen sensors at the crossroad of metabolism. Cell Metab. *9*, 11–22.

Arany, Z., Huang, L.E., Eckner, R., Bhattacharya, S., Jiang, C., Goldberg, M.A., Bunn, H.F., and Livingston, D.M. (1996). An essential role for p300/CBP in the cellular response to hypoxia. Proc. Natl. Acad. Sci. USA *93*, 12969–12973.

Beyer, S., Kristensen, M.M., Jensen, K.S., Johansen, J.V., and Staller, P. (2008). The histone demethylases JMJD1A and JMJD2B are transcriptional targets of hypoxia-inducible factor HIF. J. Biol. Chem. *283*, 36542–36552.

Bonkhoff, H. (1998). Neuroendocrine cells in benign and malignant prostate tissue: Morphogenesis, proliferation, and androgen receptor status. Prostate Suppl. *8*, 18–22.

Chiaverotti, T., Couto, S.S., Donjacour, A., Mao, J.H., Nagase, H., Cardiff, R.D., Cunha, G.R., and Balmain, A. (2008). Dissociation of epithelial and neuroendocrine carcinoma lineages in the transgenic adenocarcinoma of mouse prostate model of prostate cancer. Am. J. Pathol. *172*, 236–246.

Cindolo, L., Cantile, M., Vacherot, F., Terry, S., and de la Taille, A. (2007). Neuroendocrine differentiation in prostate cancer: from lab to bedside. Urol. Int. *79*, 287–296.

Cirillo, L.A., Lin, F.R., Cuesta, I., Friedman, D., Jarnik, M., and Zaret, K.S. (2002). Opening of compacted chromatin by early developmental transcription factors HNF3 (FoxA) and GATA-4. Mol. Cell *9*, 279–289.

Deeble, P.D., Murphy, D.J., Parsons, S.J., and Cox, M.E. (2001). Interleukin-6- and cyclic AMP-mediated signaling potentiates neuroendocrine differentiation of LNCaP prostate tumor cells. Mol. Cell. Biol. *21*, 8471–8482.

Deng, X., Liu, H., Huang, J., Cheng, L., Keller, E.T., Parsons, S.J., and Hu, C.D. (2008). Ionizing radiation induces prostate cancer neuroendocrine differentiation through interplay of CREB and ATF2: implications for disease progression. Cancer Res. *68*, 9663–9670.

Emerling, B.M., Weinberg, F., Liu, J.L., Mak, T.W., and Chandel, N.S. (2008). PTEN regulates p300-dependent hypoxia-inducible factor 1 transcriptional activity through Forkhead transcription factor 3a (FOXO3a). Proc. Natl. Acad. Sci. USA *105*, 2622–2627.

Erbel, P.J., Card, P.B., Karakuzu, O., Bruick, R.K., and Gardner, K.H. (2003). Structural basis for PAS domain heterodimerization in the basic helix-loop-helix-PAS transcription factor hypoxia-inducible factor. Proc. Natl. Acad. Sci. USA *100*, 15504–15509.

Eun, B., Lee, Y., Hong, S., Kim, J., Lee, H.W., Kim, K., Sun, W., and Kim, H. (2008). Hes6 controls cell proliferation via interaction with cAMP-response element-binding protein-binding protein in the promyelocytic leukemia nuclear body. J. Biol. Chem. *283*, 5939–5949.

Foster, B.A., Gingrich, J.R., Kwon, E.D., Madias, C., and Greenberg, N.M. (1997). Characterization of prostatic epithelial cell lines derived from transgenic adenocarcinoma of the mouse prostate (TRAMP) model. Cancer Res. *57*, 3325–3330.

Frew, I.J., Hammond, V.E., Dickins, R.A., Quinn, J.M., Walkley, C.R., Sims, N.A., Schnall, R., Della, N.G., Holloway, A.J., Digby, M.R., et al. (2003). Generation and analysis of Siah2 mutant mice. Mol. Cell. Biol. *23*, 9150–9161.

Fukuba, H., Takahashi, T., Jin, H.G., Kohriyama, T., and Matsumoto, M. (2008). Abundance of aspargynyl-hydroxylase FIH is regulated by Siah-1 under normoxic conditions. Neurosci. Lett. *433*, 209–214.

Gingrich, J.R., Barrios, R.J., Morton, R.A., Boyce, B.F., DeMayo, F.J., Finegold, M.J., Angelopoulou, R., Rosen, J.M., and Greenberg, N.M. (1996). Metastatic prostate cancer in a transgenic mouse. Cancer Res. *56*, 4096–4102.

Gustafsson, M.V., Zheng, X., Pereira, T., Gradin, K., Jin, S., Lundkvist, J., Ruas, J.L., Poellinger, L., Lendahl, U., and Bondesson, M. (2005). Hypoxia requires notch signaling to maintain the undifferentiated cell state. Dev. Cell *9*, 617–628.

Hirano, D., Jike, T., Okada, Y., Minei, S., Sugimoto, S., Yamaguchi, K., Yoshikawa, T., Hachiya, T., Yoshida, T., and Takimoto, Y. (2005). Immunohistochemical and ultrastructural features of neuroendocrine differentiated carcinomas of the prostate: an immunoelectron microscopic study. Ultrastruct. Pathol. *29*, 367–375.

Hofbauer, K.H., Gess, B., Lohaus, C., Meyer, H.E., Katschinski, D., and Kurtz, A. (2003). Oxygen tension regulates the expression of a group of procollagen hydroxylases. Eur. J. Biochem. *270*, 4515–4522.

House, C.M., Frew, I.J., Huang, H.L., Wiche, G., Traficante, N., Nice, E., Catimel, B., and Bowtell, D.D. (2003). A binding motif for Siah ubiquitin ligase. Proc. Natl. Acad. Sci. USA *100*, 3101–3106.

Huss, W.J., Gregory, C.W., and Smith, G.J. (2004). Neuroendocrine cell differentiation in the CWR22 human prostate cancer xenograft: association with tumor cell proliferation prior to recurrence. Prostate *60*, 91–97.

Huss, W.J., Gray, D.R., Tavakoli, K., Marmillion, M.E., Durham, L.E., Johnson, M.A., Greenberg, N.M., and Smith, G.J. (2007). Origin of androgen-insensitive poorly differentiated tumors in the transgenic adenocarcinoma of mouse prostate model. Neoplasia *9*, 938–950.

Ivan, M., Kondo, K., Yang, H., Kim, W., Valiando, J., Ohh, M., Salic, A., Asara, J.M., Lane, W.S., and Kaelin, W.G., Jr. (2001). HIFalpha targeted for VHL-mediated destruction by proline hydroxylation: Implications for O2 sensing. Science *292*, 464–468.

Kaidi, A., Williams, A.C., and Paraskeva, C. (2007). Interaction between beta-catenin and HIF-1 promotes cellular adaptation to hypoxia. Nat. Cell Biol. *9*, 210–217.

Kasper, L.H., Boussouar, F., Boyd, K., Xu, W., Biesen, M., Rehg, J., Baudino, T.A., Cleveland, J.L., and Brindle, P.K. (2005). Two transactivation mechanisms cooperate for the bulk of HIF-1-responsive gene expression. EMBO J. *24*, 3846–3858.

Loh, Y.H., Zhang, W., Chen, X., George, J., and Ng, H.H. (2007). Jmjd1a and Jmjd2c histone H3 Lys 9 demethylases regulate self-renewal in embryonic stem cells. Genes Dev. *21*, 2545–2557.

Makino, Y., Kanopka, A., Wilson, W.J., Tanaka, H., and Poellinger, L. (2002). Inhibitory PAS domain protein (IPAS) is a hypoxia-inducible splicing variant of the hypoxia-inducible factor-3alpha locus. J. Biol. Chem. *277*, 32405–32408.

Mirosevich, J., Gao, N., Gupta, A., Shappell, S.B., Jove, R., and Matusik, R.J. (2006). Expression and role of Foxa proteins in prostate cancer. Prostate *66*, 1013–1028.

Moller, A., House, C.M., Wong, C.S., Scanlon, D.B., Liu, M.C., Ronai, Z., and Bowtell, D.D. (2009). Inhibition of Siah ubiquitin ligase function. Oncogene *28*, 289–296.

Monsef, N., Helczynski, L., Lundwall, A., and Pahlman, S. (2007). Localization of immunoreactive HIF-1alpha and HIF-2alpha in neuroendocrine cells of both benign and malignant prostate glands. Prostate *67*, 1219–1229.

Nakayama, K., Frew, I.J., Hagensen, M., Skals, M., Habelhah, H., Bhoumik, A., Kadoya, T., Erdjument-Bromage, H., Tempst, P., Frappell, P.B., et al. (2004). Siah2 regulates stability of prolyl-hydroxylases, controls HIF1alpha abundance, and modulates physiological responses to hypoxia. Cell *117*, 941–952.

Nakayama, K., Qi, J., and Ronai, Z. (2009). The ubiquitin ligase Siah2 and the hypoxia response. Mol. Cancer Res. *7*, 443–451.

Nowak, J.A., Polak, L., Pasolli, H.A., and Fuchs, E. (2008). Hair follicle stem cells are specified and function in early skin morphogenesis. Cell Stem Cell *3*, 33–43.

Qi, J., Nakayama, K., Gaitonde, S., Goydos, J.S., Krajewski, S., Eroshkin, A., Bar-Sagi, D., Bowtell, D., and Ronai, Z. (2008). The ubiquitin ligase Siah2 regulates tumorigenesis and metastasis by HIF-dependent and -independent pathways. Proc. Natl. Acad. Sci. USA *105*, 16713–16718.

Ruas, J.L., Berchner-Pfannschmidt, U., Malik, S., Gradin, K., Fandrey, J., Roeder, R.G., Pereira, T., and Poellinger, L. (2010). Complex regulation of the transactivation function of hypoxia-inducible factor-1 alpha by direct interaction with two distinct domains of the CREB-binding protein/p300. J. Biol. Chem. *285*, 2601–2609.

Schmidt, R.L., Park, C.H., Ahmed, A.U., Gundelach, J.H., Reed, N.R., Cheng, S., Knudsen, B.E., and Tang, A.H. (2007). Inhibition of RAS-mediated transformation and tumorigenesis by targeting the downstream E3 ubiquitin ligase seven in absentia homologue. Cancer Res. *67*, 11798–11810.

Sella, A., Konichezky, M., Flex, D., Sulkes, A., and Baniel, J. (2000). Low PSA metastatic androgen- independent prostate cancer. Eur. Urol. *38*, 250–254.

Semenza, G.L. (2003). Targeting HIF-1 for cancer therapy. Nat. Rev. Cancer *3*, 721–732.

Shah, R.B., Mehra, R., Chinnaiyan, A.M., Shen, R., Ghosh, D., Zhou, M., Macvicar, G.R., Varambally, S., Harwood, J., Bismar, T.A., et al. (2004). Androgen-independent prostate cancer is a heterogeneous group of diseases: lessons from a rapid autopsy program. Cancer Res. *64*, 9209–9216.

Shimizu, S., Kumagai, J., Eishi, Y., Uehara, T., Kawakami, S., Takizawa, T., and Koike, M. (2007). Frequency and number of neuroendocrine tumor cells in prostate cancer: no difference between radical prostatectomy specimens from patients with and without neoadjuvant hormonal therapy. Prostate *67*, 645–652.

Sotomayor, P., Godoy, A., Smith, G.J., and Huss, W.J. (2009). Oct4A is expressed by a subpopulation of prostate neuroendocrine cells. Prostate *69*, 401–410.

Sramkoski, R.M., Pretlow, T.G., 2nd, Giaconia, J.M., Pretlow, T.P., Schwartz, S., Sy, M.S., Marengo, S.R., Rhim, J.S., Zhang, D., and Jacobberger, J.W. (1999). A new human prostate carcinoma cell line, 22Rv1. In Vitro Cell. Dev. Biol. Anim. *35*, 403–409.

Vias, M., Massie, C.E., East, P., Scott, H., Warren, A., Zhou, Z., Nikitin, A.Y., Neal, D.E., and Mills, I.G. (2008). Pro-neural transcription factors as cancer markers. BMC Med. Genomics *1*, 17.

Wang, H., Leav, I., Ibaragi, S., Wegner, M., Hu, G.F., Lu, M.L., Balk, S.P., and Yuan, X. (2008). SOX9 is expressed in human fetal prostate epithelium and enhances prostate cancer invasion. Cancer Res. *68*, 1625–1630.

Yuan, T.C., Veeramani, S., Lin, F.F., Kondrikou, D., Zelivianski, S., Igawa, T., Karan, D., Batra, S.K., and Lin, M.F. (2006). Androgen deprivation induces human prostate epithelial neuroendocrine differentiation of androgen-sensitive LNCaP cells. Endocr. Relat. Cancer *13*, 151–167.

Zhang, H., Gao, P., Fukuda, R., Kumar, G., Krishnamachary, B., Zeller, K.I., Dang, C.V., and Semenza, G.L. (2007). HIF-1 inhibits mitochondrial biogenesis and cellular respiration in VHL-deficient renal cell carcinoma by repression of C-MYC activity. Cancer Cell *11*, 407–420.

Zhou, Z., Flesken-Nikitin, A., Corney, D.C., Wang, W., Goodrich, D.W., Roy-Burman, P., and Nikitin, A.Y. (2006). Synergy of p53 and Rb deficiency in a conditional mouse model for metastatic prostate cancer. Cancer Res. *66*, 7889–7898.